# A Multilevel Bidirectional Four-Port DC-DC Converter to Create a DC-Grid in Solid-State Transformers with Hybrid AC/DC Grids

Vitor Monteiro
*Centro ALGORITMI*
*University of Minho*
Guimaraes, Portugal
vmonteiro@dei.uminho.pt

Catia Oliveira
*Centro ALGORITMI*
*University of Minho*
Guimaraes, Portugal
c.oliveira@dei.uminho.pt

Joao L. Afonso
*Centro ALGORITMI*
*University of Minho*
Guimaraes, Portugal
jla@dei.uminho.pt

***Abstract*—Smart grids are incessantly contemplating new challenges about power electronics technologies, and this paper focuses on the application of solid-state transformers (SSTs) and the forthcoming perspective of hybrid AC/DC grids. In such perspective, a multilevel bidirectional four-port (MB4P) DC-DC converter is proposed to be integrated in a three-phase SST. It interfaces the SST through three independently ports, corresponding to the three-phases, and the other port is used to create a DC grid. The proposed MB4P DC-DC converter has as main features a multilevel operation with seven voltage levels as function of the voltages on both DC sides, as well as the interleaved operation, where the controlled variables have a ripple with a frequency six times higher than the switching frequency. Furthermore, it can operate in buck or boost modes, and with current or voltage control. Besides the voltage and current control, specific attention is given to the proposed PWM. The advanced attributes of the MB4P DC-DC converter are proven by computer simulations and by analytical description, both exploring steady-state and transient-state distinctive requirements.**

***Keywords*—DC-DC Converter, Solid-State Transformer, Hybrid AC/DC Grid, Multilevel, Interleaved, Bidirectional.**

## I. INTRODUCTION

Smart grids are a reality and are in constant development due to the presently energy concerns and the emerging technologies that are being integrated, as well as the new paradigms of on-grid and off-grid power grids, where electric vehicles and renewables are boosting technologies for such development [1][2][3]. This is even more applicable to encompass smart cities inside smart grids [4]. Moreover, examining in detail such development, it is identified as a common technology the power electronics [5][6]. However, since more and more power electronics solutions are used into the power grids, the controllability of power quality is even more relevant in the perspective of smart grids [7]. Summarizing, the use of power electronics solutions in modern power grids includes: solid-state transformers (SST) [8]; electric mobility [9]; renewables [10]; DC microgrids [11]; hybrid AC/DC grids [12]; and enhanced control of converters and topologies [13][14]. Particularizing, as exposed principally in last decade, SST are used for miscellaneous applications [15][16][17]. The pertinence of SST for forthcoming grids is introduced in [18], a revision of SST including crucial characteristics is presented in [19], a comprehensive review regarding of SST is available in [20], an SST connecting renewables and electric vehicles is debated in [21], a DCSST interfacing renewable sources in introduced in [22], and SST interfacing photovoltaic and wind power systems are presented in [23][24]. Typically, a SST is constituted by three power stages: an AC-DC converter; an isolated DC-DC converter; and a DC-AC converter [25][26][27]. As aforementioned, the possibility of the SST to interface technologies natively operating in DC, such as renewables and storage systems, is a valuable feature. Therefore, an additional DC-DC converter must be considered in the design of the SST, forming a hybrid AC/DC power grid on the secondary-side [28]. In such case, typically, the DC-DC converter is linked to the output of the isolated DC-DC converters. In a three-phase architecture of SST with three individual isolated DC-DC converters, the DC-DC converter used to create the DC grid must be designed with three interfaces in a DC side and with a single interface in the other DC side. The DC-DC converter is fundamental to accomplish with the requirements of voltage and current of the DC grid, permitting to establish a buck or boost operation [29].

In this context, this paper proposes a specific DC-DC converter to be integrated in a hybrid AC/DC SST. As main three distinguished features of the proposed DC-DC converter can be highlighted: multilevel; bidirectional; and four-port. Therefore, it is identified as multilevel bidirectional four-port (MB4P) DC-DC converter. The application of the proposed MB4P DC-DC converter framed in an SST is presented in Fig. 1. As shown, the three-ports are directly connect to the secondary-side of the isolated DC-DC converters, each port linked to each phase of the SST, while the other port is used to form the DC grid. Obviously, other DC-DC converters can be used to integrate the hybrid AC/DC SST, but not presenting the features of the proposed MB4P DC-DC converter, namely in terms of multilevel and interleaved features as following described. As distinguishing aspects, it can be emphasized: (a) four-ports distributed in two DC sides, where one of the DC sides has three-ports to interface a balanced three-phase system, while the other DC side has a single DC port; (b) each of the three-ports has a split DC-link, which is used to obtain the multilevel feature; (c) the three-ports are individually controlled and are independently, i.e., each port is connected to

each phase of the SST and must be voltage balanced; (d) the DC-DC converter can be bidirectional controlled in buck or boost mode, as well as with current or voltage control; (e) multilevel operation producing seven voltage levels as function of the voltages on both DC sides and, in transient-state, permitting to reach the reference faster than the traditional DC-DC converters; (f) interleaved operation, where the controlled variable has a ripple with a frequency six times higher than the switching frequency; (g) all of the previous aspects can be combined and are independently of the buck or boost mode.

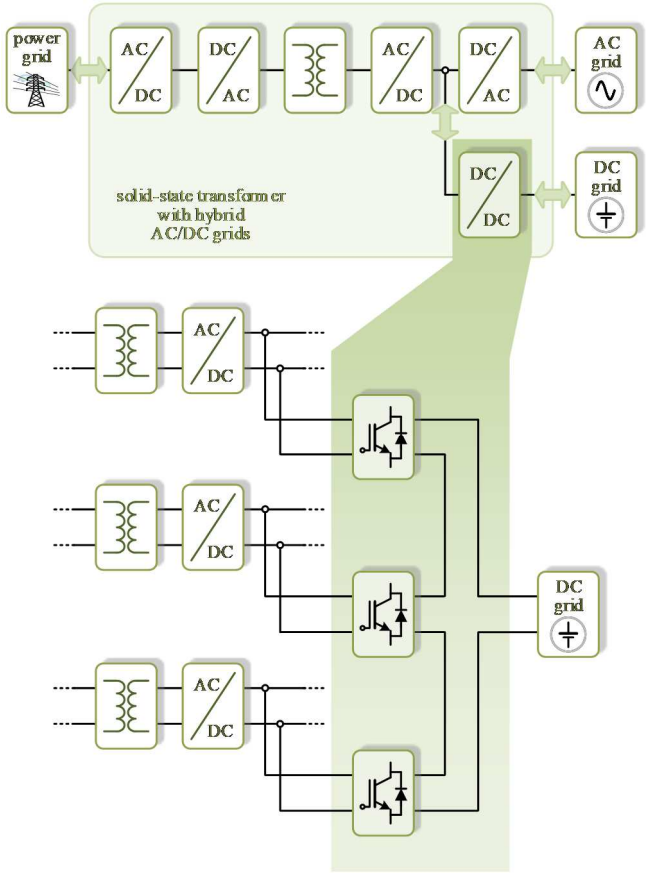


Fig. 1. Traditional structure of solid-state transformer (SST) constituted by three power stages (AC-DC converter, isolated DC-DC converter and DC-AC converter) and the application of the proposed MB4P DC-DC converter framed in the SST.

As previously mentioned, the proposed MB4P DC-DC converter is dedicated to being integrated in applications of SST to create a DC grid aiming to form a hybrid AC/DC structure (therefore, various technologies can be interfaced, such as energy storage systems or charging systems for electric mobility). The proposed MB4P DC-DC converter is presented in Fig. 2, which is formed by 12 switching devices divided by the three-phases. The operation principle of the proposed MB4P DC-DC converter is introduced in section II, while the voltage and current control and the modulation in section III. The validation of the main features both in steady/transient state and in buck/boost mode are presented in section IV. The conclusions are summarized in section V.

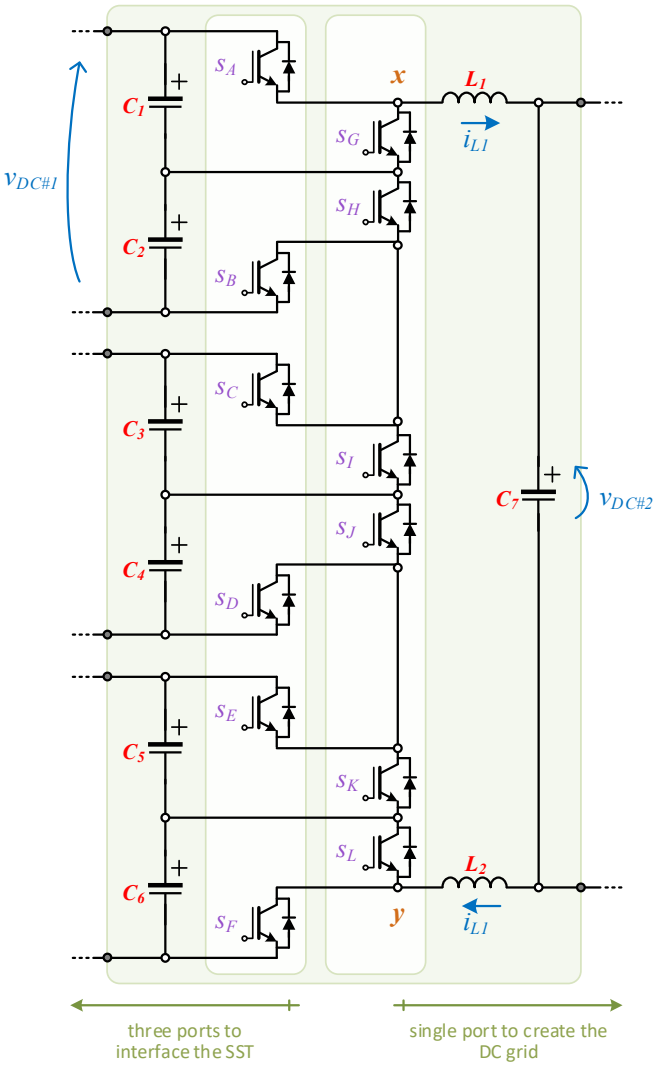


Fig. 2. Topology of the proposed MB4P DC-DC converter, highlighting the three independently ports to interface the SST and the single port to establish the DC grid.

## II. Proposed Converter: Principle of Operation

As exhibited in Fig. 2, the MB4P DC-DC converter is formed by 12 switching devices and it is categorized as symmetrical due to the voltage symmetry. In terms of operation, the MB4P DC-DC converter operates in bidirectional mode, exchanging power between the SST and the DC grid. In buck-mode (with power from the SST to the DC grid) are only used the switching devices $s_A$ to $s_F$, while in boost-mode (with power from the DC grid to the SST) are only used the switching devices $s_G$ to $s_L$.

The switching devices are individual controlled to guarantee the mentioned key features, therefore, are considered individual carriers to control each switching device with fixed switching frequency, but it is considered a single reference to be compared with the carriers. The carriers are strategic shifted targeting to control the variable like the operation of a traditional interleaved converter. However, it is important to

note that the proposed converter is not constituted by the parallel of DC-DC converter as an interleaved converter.

In the context of operation framed with the SST, the power is exchanged in a balanced way by the three-phases on the SST side. Even if for some reason the voltages are not properly balanced, this situation does not affect the operation of the proposed converter in terms of the DC grid.

The average value of the current in $s_A$ to $s_F$ and the average value of current in $s_G$ to $s_L$ is determined, respectively, by:

$$\overline{i}_{S\{A,B,C,D,E,F\}} = \overline{i_{L\{1,2\}}} - \frac{1}{3}\ \overline{i_{L\{1,2\}}}\ \frac{v_{DC\#1}}{v_{DC\#2}}, \tag{1}$$

$$\overline{i}_{S\{G,H,I,J,K,L\}} = \frac{1}{3}\ \overline{i_{L\{1,2\}}}\ \frac{v_{DC\#1}}{v_{DC\#2}}. \tag{2}$$

Regarding the average value of the voltage in $s_A$ to $s_F$ and the average value of the voltage in $s_G$ to $s_L$ it is determined, respectively, by:

$$\overline{v}_{S\{A,B,C,D,E,F\}} = \frac{1}{2}\ v_{DC\#1} - \frac{1}{6} v_{DC\#2}\ , \tag{3}$$

$$\overline{v}_{S\{G,H,I,J,K,L\}} = \frac{1}{4}\ v_{DC\#1} - \frac{1}{12} v_{DC\#2}\ . \tag{4}$$

Through an examination of the presented equations, when the objective is to guarantee the most balancing strategy of voltages and currents, a value of voltage in the DC side DC#2 close to half of the total voltage in the DC side DC#1 (i.e., the sum of the three independent voltages) must be considered. This situation can be achieved by adjusting the voltage values on each DC side, e.g., it can be beneficial to increase the voltage on one DC side by forcing the converter to operate in such situation.

## III. Proposed Converter: Control and Pulse-Width Modulation

As previously mentioned, the proposed MB4P DC-DC converter has two DC sides, identified as DC#1 and DC#2, which can be controlled independently. Since the objective is the integration into a three-phase SST, one of the DC sides (DC#1) is controlled with voltage feedback by the SST. Consequently, the DC side DC#2 can be controlled with voltage feedback in buck-mode, or with current feedback in buck or boost mode, permitting to establish a bidirectional power flow between the SST and the DC grid. Such possibilities of control are explored as follows.

### A. Buck Operation with Current Control

Analyzing the converter in buck-mode, where the source is in the DC side DC#1 and the load is in the DC side DC#2, the distinct voltages are listed as follows:

$$v_{xy}(t) = v_{DC\#2}(t) + v_{L1}(t) + v_{L2}(t)\ . \tag{5}$$

As shown, such relation contemplate the operating voltage of the converter ($v_{xy}$), the output voltage ($v_{DC\#2}$), and the voltage in $L_{1,2}$ ($v_{L\{1,2\}}$). Knowing that the voltage across $L_{1,2}$ is function of its current, the previous equation can be rewritten as:

$$v_{xy}(t) = v_{dc\#2}(t) + \frac{L_1\ di_{L1}(t)}{dt} + \frac{L_2\ di_{L2}(t)}{dt}. \tag{6}$$

The digital implementation, using the forward Euler discrete implementation, can be obtained from:

$$v_{xy}[k] = v_{dc\#2}[k] + L_{\{1,2\}}\ {T_s}^{-1}\left(i_{L\{1,2\}}[k+1] - i_{L\{1,2\}}[k]\right). \tag{7}$$

The current in [$k$+1] must be the current throughout [$k$, $k$+1], consequently, as a substitute of $i_{L\{1,2\}}[k+1]$ must be contemplated the reference. For such purpose, $v_{xy}[k]$ is the variable that is compared with the carrier, forcing to control the current throughout [$k$, $k$+1]. The MB4P DC-DC converter is controlled by a single current, differently from a traditional interleaved converter, but it has the same functionally of obtaining a variable with a ripple whose frequency is multiple of the switching frequency. Therefore, it is considered a single control variable, in this case $v_{xy}[k]$, but it is compared with 6 individual carriers shifted by 60 degrees, all of them with the same amplitude and frequency. The output of the comparison is used to control the switching devices $s_A$ to $s_F$ while the switching devices $s_G$ to $s_L$ are maintained off (this is valid during the buck-mode).

### B. Buck Operation with Voltage Control

With the objective of controlling the converter with voltage feedback, a direct relation can be recognized as:

$$v_{DC\#2} = \frac{1}{6}\frac{v_{DC\#1}}{v_{DC\#2}}\left(v_{dc\#1,1} + v_{dc\#1,2}\right). \tag{8}$$

### C. Boost Operation with Current Control

Analyzing the converter in boost-mode, where the source is in the DC side DC#2 and the load is in the DC side DC#1, the distinct voltages are listed as follows:

$$v_{xy}(t) = -v_{DC\#2}(t) + v_{L1}(t) + v_{L2}(t)\ , \tag{9}$$

As shown, it is possible to recognize similarities with the buck-mode, therefore, the final digital implementation is:

$$v_{xy}[k] = -v_{DC\#2}[k] + L_{\{1,2\}}{T_s}^{-1}\left(i_{L\{1,2\}}[k+1] - i_{L\{1,2\}}[k]\right). \tag{10}$$

The performed analysis for the buck-mode is also applied to the boost-mode, i.e., is considered a single variable to be compared with six carriers, all of them with the same amplitude and frequency and shifted 60 degrees. The output of the comparison is used to control the switching devices $s_G$ to $s_L$ while the switching devices $s_A$ to $s_F$ are maintained off (this is valid during the boost-mode).

### D. Boost Operation with Voltage Control

The objective of the proposed MB4P DC-DC converter is to be integrated into a three-phase SST, therefore, the voltage control of the interface DC#1 is guaranteed by the SST. However, if the converter is used in other applications, it can also be controlled by voltage, therefore, it can be established:

$$\frac{1}{2}\left(v_{dc\#1,1} + v_{dc\#1,2}\right) = \frac{v_{dc\#2}}{(1-D)}. \tag{11}$$

## IV. Proposed Converter: Validation of Operation Modes

The validation was performed with a developed PSIM model and contemplating realistic requirements. Each

switching device is controlled with a frequency of 20 kHz, but the control is executed at twice of such frequency. The voltage on the DC side of the grid was considered as variable, from 0 V to 1200 V, while the power was considered as variable from 0 W to 24 kW. These voltage levels are only exemplificative to demonstrate the capabilities of the converter and are suitable for residential and commercial DC nano grids. The voltage on each port used in the interface of the SST was considered with a value of 400 V (considering a split DC-link, each part with 200 V). Additionally, were considered inductors with a value of 500 µH and capacitors with a value of 100 µF.

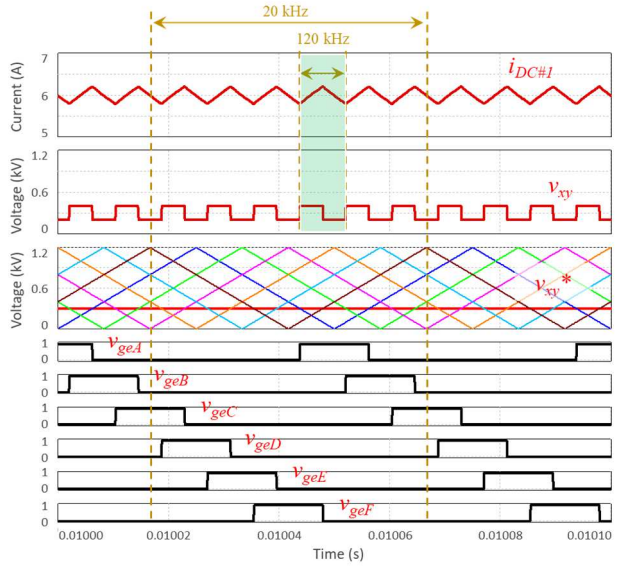


Fig. 3. Validation during the buck-mode in steady-state with a fixed duty-cycle of 25%, showing the influence of the duty-cycle value on the current ripple: current on the DC side DC#1 ($i_{DC\#1}$); voltage of the converter ($v_{xy}$); reference ($v_{xy}$*) and carriers used to control the switching devices; control signals of the switching devices ($v_{geA}$, $v_{geB}$, $v_{geC}$, $v_{geD}$, $v_{geE}$, $v_{geF}$).

An exemplary result is shown in Fig. 3 during the buck-mode, in which a fixed duty-cycle value of 25% was considered. This result allows to visualize the influence of this duty-cycle value on the current ripple. Thus, this figure shows the current, the operating voltage of the converter, all carriers that allow the control of all switching devices during buck-mode, as well as the control signals of the IGBTs. As can be seen, 6 carriers are required, and they are properly out of phase with each other. As there are 6 carriers, the shift between them is 60 degrees. Therefore, the control signals of the IGBTs show the same control shift. As the switching devices are controlled with a switching frequency of 20 kHz, the current ripple has a frequency that corresponds to 6 times more, specifically, a frequency of 120 kHz. This feature is very relevant since it is possible to significantly reduce the coupling filter when comparing with tradition buck converters. In this situation, as the duty-cycle is 25% and the output voltage is less than half the voltage of one of the DC-links, it results in an operating voltage of the converter with values of 200 V and 400 V.

Fig. 4 shows, in more detail, the current ripple as a function of the control signals of the switching devices. As can be seen, when only one of the switching devices is in the on state, the operating voltage of the converter assumes the value of 600 V. Obviously these values depend on the values of the output voltage and the voltage of each DC-link, which is necessarily influenced by the duty-cycle value. This result permits to verify the influence of the duty-cycle on the ripple of the current. Since a duty-cycle value of 50% was considered, it is verified that the current ripple is canceled, illustrating the operation like a traditional interleaved converter (but only requiring the control of a single variable).

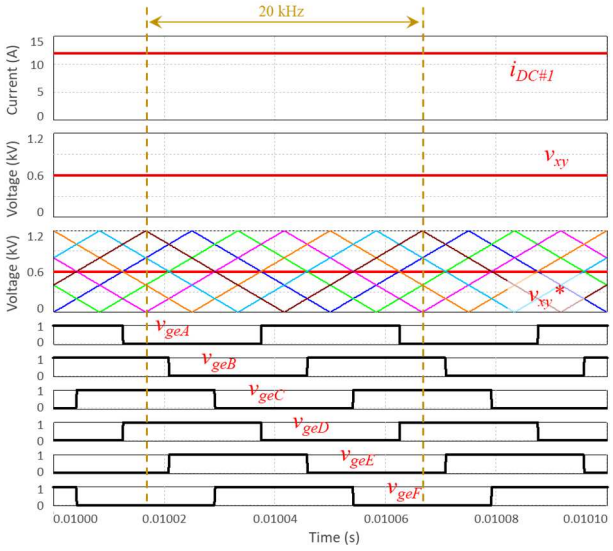


Fig. 4. Validation during the buck-mode in steady-state with a fixed duty-cycle of 50%, showing the influence of the duty-cycle value on the current ripple: on the DC side DC#1 ($i_{DC\#1}$); voltage of the converter ($v_{xy}$); reference ($v_{xy}$*) and carriers used to control the switching devices; control signals of the switching devices ($v_{geA}$, $v_{geB}$, $v_{geC}$, $v_{geD}$, $v_{geE}$, $v_{geF}$).

Fig. 5 shows a result of the current and the operating voltage of the converter, considering a fixed value of resistive load. In this way, it is possible to verify that by increasing the operating current, i.e., by changing the current reference, the output voltage also increases, forcing the operating voltage of the converter to also assume different values. In this case, as it turns out, the current increased from a value of 0 A to a value of 22 A, and the operating voltage assumed all possible values, according to the value of half the voltage of each DC-link, i.e., 0 V, 200 V, 400 V, 600 V, 800 V, 1000 V and 1200 V. This result is illustrative when the DC output voltage varies, which can happen, e.g., when a battery is connected to the DC side DC#2 of the converter. In this case, e.g., the converter could only be used to interface an energy storage system.

Fig. 6 shows the detail of the current and the operating voltage, demonstrating that the current ripple is null during the transition between voltage levels. Obviously, specific control strategies can be used to minimize the ripple, mainly through the adjust of the voltage on the DC sides. Fig. 7 shows a result in transient-state that allows visualizing the dynamic operation of the converter. In this case, a variation from 10 A to 20 A was considered, and the operating voltage varied due to the fixed value of the load. In this case, the operating voltage varied between 400 V and 600 V and after the sudden variation of the operating current, the voltage started to vary between 800 V and 1000 V. As a curiosity, as the voltage on the DC side DC#2

became 1000 V, the duty-cycle is 50%, allowing to cancel the current ripple, as can be seen.

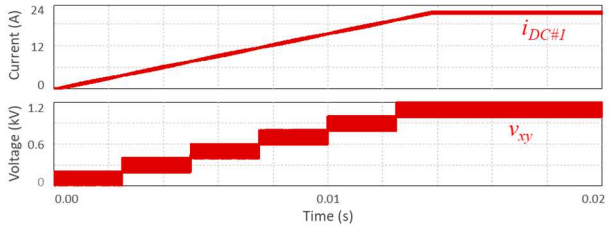


Fig. 5. Validation during the buck-mode showing the current ($i_{DC\#1}$) and the voltage ($v_{xy}$) of the converter, increasing the operating current to force the voltage of the converter to assume all different possible values (i.e., 0 V, 200 V, 400 V, 600 V, 800 V, 1000 V and 1200 V).

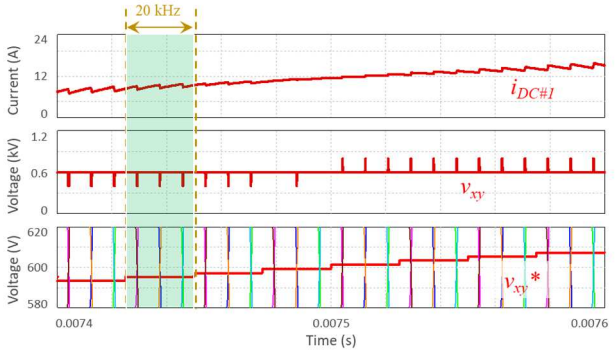


Fig. 6. Validation during the buck-mode showing in detail the current ($i_{DC\#1}$), the voltage ($v_{xy}$), reference ($v_{xy}$*) and the carriers used to control the switching devices, demonstrating that the current ripple is null during the transition between voltage levels.

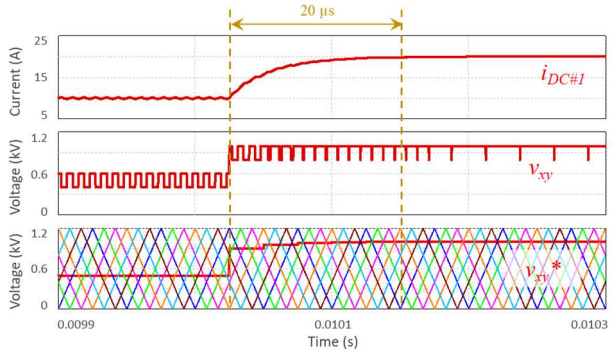


Fig. 7. Validation during the buck mode in transient-state, from an operating current from 10 A to 20 A, showing the current ($i_{DC\#1}$), the voltage ($v_{xy}$), the reference ($v_{xy}$*) and carriers used to control the switching devices.

Fig. 8 shows a result that allows to validate the boost-mode. In this result, the current assumes a negative value only due to the position of the sensor (i.e., a position contrary to the buck-mode). This result was obtained with current control, in this case, imposing a reference value of 10 A. The operating power is 3 kW, with the voltage on the DC side DC#2 being 300 V. As the voltage value is more than half of the voltage of one of the DC-link, the converter operates with a voltage between 200 V and 400 V. By varying the voltage on the DC side DC#2, obviously the operating voltage of the converter will also vary. Also in this result, like in the buck-mode, it is proven that the current ripple has a frequency of 120 kHz, which is six times higher than the switching frequency. As can be seen, a single control variable and six carriers are used, corresponding to the control of the switching devices $S_G$ to $S_L$. This result is illustrative of an operating situation in steady-state in which power is injected into the SST from the DC grid.

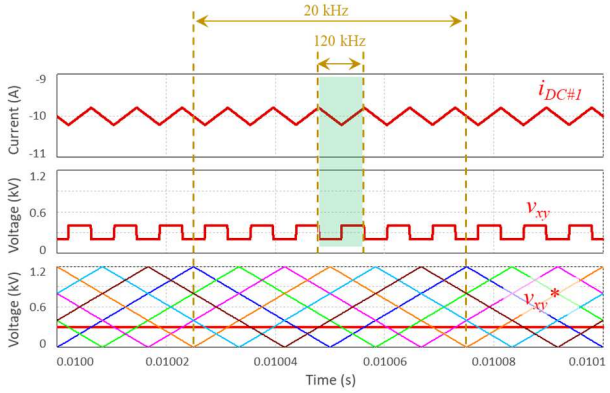


Fig. 8. Validation during the boost-mode in steady-state showing in detail the operating current ($i_{DC\#1}$), the voltage ($v_{xy}$), reference ($v_{xy}$*) and the carriers used to control the switching devices, demonstrating that the current is centered in the reference of 10 A.

Fig. 9 shows a result corresponding to the boost-mode, but in a transient-state. In this case, it was considered a fixed operating voltage on the DC side DC#2, as well as on the DC side DC#1, and a current variation from 10 A to 20 A, which corresponds to a sudden variation in the operating power of 3 kW to 6 kW. The transition takes 50 µs, and during the transition the operating voltage assumes the values of 0 V, 200 V and 400 V, allowing the converter to reach the normal operation as quickly as possible. As soon as the nominal steady-state is reached again, the operating voltage returns to only the values of 200 V and 400 V. This result illustrates an operating situation in which power is injected into the SST from the DC grid, validating the variation in transient-state and with a sudden variation, i.e., no smooth transition strategy is used. In this way it is possible to validate the dynamic behavior of the converter in boost-mode.

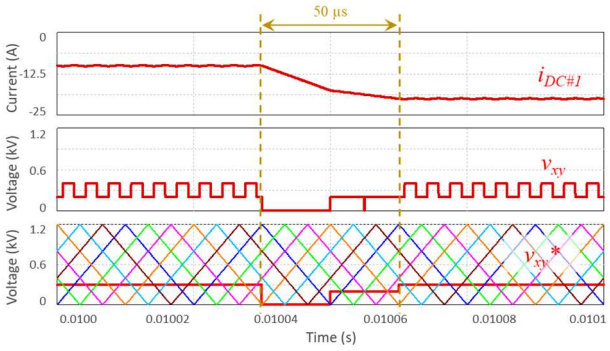


Fig. 9. Validation during the boost mode in transient-state showing in detail the operating current ($i_{DC\#1}$), the voltage ($v_{xy}$), reference ($v_{xy}$*) and the carriers used to control the switching devices, corresponding to a sudden variation in the operating power from 3 kW to 6 kW.

## V. Conclusions

Smart grids are constantly evolving, where the incorporation of solid-state transformers (SSTs) and hybrid AC/DC grids are promising and revolutionary technologies. Focusing on such technologies, a multilevel bidirectional four-port (MB4P) DC-DC converter is proposed. It is constituted by two DC sides, one of them with three ports interfacing a three-phase SST and the other port forms a DC grid. Along the paper the proposed MB4P DC-DC converter is validated under the main distinctive operation modes with the objective of demonstrating its main features. Both in buck and boost modes, it was verified the multilevel feature, highlighting how the distinctive seven voltage levels (0 V, 200 V, 400 V, 600 V, 800 V, 1000 V and 1200 V) are obtained, and the conditions of operation that forces such voltage levels. Besides, independently of the operating voltage levels, the operation in buck or boost modes, and the value of operating power (with a maximum power of 24 kW), it was verified the interleaved operation, demonstrating controlled variables with a ripple whose frequency corresponds to six times the switching frequency (6 x 20 kHz = 120 kHz). Particular detail and explanation is given to the proposed PWM, since it is fundamental to guarantee the correct operation of the MB4P DC-DC converter. Intending to achieve a practical validation, distinguishing requirements were contemplated in steady-state and transient-state to verify the dynamic comportment of the seven levels, while maintaining the interleaved feature.

## Acknowledgment

This work has been supported by FCT – Fundação para a Ciência e Tecnologia within the R&D Units Project Scope: UIDB/00319/2020. This work has been supported by the FCT Project newERA4GRIDs PTDC/EEI-EEE/30283/2017, and by the FCT Project DAIPESEV PTDC/EEI-EEE/30382/2017.

## References

[1] Vítor Monteiro, P. Lima, Tiago J. C. Sousa, Júlio S. Martins, João L. Afonso, “An Off-Board Multi-Functional Electric Vehicle Charging Station for Smart Homes: Analysis and Experimental Validation,” MDPI Energies, vol.13, no.8, pp.1-23, Abr. 2020.

[2] F. Blaabjerg, J. M. Guerrero, “Smart Grid and Renewable Energy Systems,” ICEMS International Conference on Electrical Machines and Systems, pp.1-10, Aug. 2011.

[3] A. P. Sakis Meliopoulos, George Cokkinides, Renke Huang, Evangelos Farantatos, Sungyun Choi, Yonghee Lee, Xuebei Yu, “Smart Grid Technologies for Autonomous Operation and Control,” IEEE Trans. Smart Grid, vol.2, no.1, pp.1-10, Mar. 2011.

[4] Marcelo Masera, E. Bompard, Francesco Profumo, Nouredine Hadjsaid, “Smart (Electricity) Grids for Smart Cities: Assessing Roles and Societal Impacts,” Proc. IEEE, vol.106, no.4, pp.613-625, Apr. 2018.

[5] Jing Zhang, “Power Electronics in Future Electrical Power Grid,” IEEE PEDG International Symposium on Power Electronics for Distributed Generation Systems, pp.1-3, July 2013.

[6] Ma Zhengyou, “Study on the Application of Advanced Power Electronics in Smart Grid,” IEEE FGCT International Conference on Future Generation Communication Technologies, pp.96-99, 2017.

[7] A. Luo, Q. Xu, F. Ma, Y. Chen, “Overview of Power Quality Analysis and Control Technology for the Smart Grid,” SPRINGER Journal of Modern Power Systems and Clean Energy, vol.4, pp.1-9, Jan. 2016.

[8] Jonas E. Huber, Johann W. Kolar, “Applicability of Solid-State Transformers in Today’s and Future Distribution Grids,” IEEE Trans. Smart Grid, vol.10, no.1, pp.317-326, Jan. 2019.

[9] Vitor Monteiro, J. Ferreira, A. Melendez, C. Couto, Joao L. Afonso, “Experimental Validation of a Novel Architecture Based on a Dual-Stage Converter for Off-Board Fast Battery Chargers of Electric Vehicles,” IEEE Trans. Veh. Tech., vol.67, pp.1000-1011, Feb. 2018.

[10] Vitor Monteiro, J. G. Pinto, Joao L. Afonso, “Experimental Validation of a Three-Port Integrated Topology to Interface Electric Vehicles and Renewables with the Electrical Grid”, IEEE Trans. Ind. Informat., vol.14, no.6, pp 2364-2374, June 2018.

[11] N. Bayati, A. Hajizadeh, M. Soltani, “Protection in DC microgrids: a comparative review,” IET Smart Grid, vol.1, no.3, pp.66-75, Sept. 2018.

[12] Farzam Nejabatkhah, Yun Wei Li, And Hao Tian, “Power Quality Control of Smart Hybrid AC/DC Microgrids: An Overview,” IEEE Access, vol.7, pp.52295-52318, Apr. 2019.

[13] S. Gorji, H. Sahebi, Mehran Ektesabi, And Ahmad, B. Rad, “Topologies and Control Schemes of Bidirectional DC–DC Power Converters: An Overview,” IEEE ACCESS, vol.7, pp117997-118019, Aug. 2019.

[14] Juan David Paez, David Frey, Jose Maneiro, Seddik Bacha, Piotr Dworakowski, “Overview of DC–DC Converters Dedicated to HVdc Grids,” IEEE Trans. Power Del., vo.34, no.1, pp.119-128, Feb. 2019.

[15] Y. Ko, A. Chub, L. Costa, M. Andresen, M. Liserre, “Smart transformer universal operation,” IEEE APEC Applied Power Electronics Conference and Exposition, pp.1609-1616, San Antonio, TX, Apr. 2018.

[16] Harish S. Krishnamoorthy, P. Enjeti, Jose J. Sandoval, “Solid State Transformer for Grid Interface of High-Power Multi-Pulse Rectifiers,” IEEE Trans. Ind. Appl., vol.54, no.5, pp.5504-5511, Dec. 2017.

[17] Arun Chandrasekharan Nair. B. G. Fernandes, “A novel multi-port solid state transformer enabled isolated hybrid microgrid architecture,” IEEE IECON Annual Conference of the Industrial Electronics Society, Beijing, pp.651-656, Nov. 2017.

[18] Jonas E. Huber, Johann W. Kolar, “Applicability of Solid-State Transformers in Today’s and Future Distribution Grids,” IEEE Trans. Smart Grid, vol.10, no.1, pp.317-326, Jan. 2019.

[19] M. A. Hannan et al., "State of the Art of Solid-State Transformers: Advanced Topologies, Implementation Issues, Recent Progress and Improvements," in IEEE Access, vol. 8, pp. 19113-19132, 2020.

[20] J. E. Huber, J. W. Kolar, “Solid-State Transformers: On the Origins and Evolution of Key Concepts,” in IEEE Industrial Electronics Magazine, vol. 10, no. 3, pp. 19-28, Sept. 2016.

[21] Q. Chen, N. Liu, C. Hu, L. Wang, J. Zhang, “Autonomous Ener-gy Management Strategy for Solid-State Transformer to Integrate PV-Assisted EV Charging Station Participating in Ancillary Service,” IEEE Trans. Ind. Informat., vol.13, no.1, pp.258-269, Feb. 2017.

[22] H. Shi, H. Wen, Y. Hu, Y. Yang, Y. Wang, “Efficiency Optimization of DC Solid-State Transformer for Photovoltaic Power Systems,” IEEE Trans. Ind. Electron., vol.67, no.5, pp.3583-3595, May 2020.

[23] H. Zhao, T. Zhu, D. Cheng, B. Li, J. Ding, Y. Li, “Research on the smart modular cascaded solid-state transformer interfaced to distributed photovoltaic power generation system,” IEEE The Journal of Engineering, vol.2017, no.13, pp.1872-1879, 2017.

[24] I. Syed, V. Khadkikar, “Replacing the Grid Interface Transformer in Wind Energy Con-version System with Solid-State Transformer,” IEEE Trans. Power Sys., vol.32, no.3, pp.2152-2160, May 2017.

[25] H. Chen, D. Divan, “Design of a 10-kV·A Soft-Switching Solid-State Transformer (S4T),” IEEE Trans. Power Electron., vol.33, no.7, pp.5724-5738, July 2018.

[26] J. E. Huber, J. Böhler, D. Rothmund, J. W. Kolar, “Analysis and cell-level experimental verification of a 25 kW all-SiC isolated front end 6.6 kV/400 V AC-DC solid-state transform-er,” CPSS Trans. On Power Electronics and Applications, vol.2, no.2, pp.140-148, Aug. 2017.

[27] L. A. Garcia Rodriguez, V. Jones, A. R. Oliva, A. Escobar-Mejía, J. C. Balda, “A New SST Topology Comprising Boost Three-Level AC/DC Converters for Applications in Electric Power Distribution Systems,” IEEE J. Emerg. Sel. Topics Power Electron., vol.5, no.2, pp.735-746, June 2017.

[28] Vítor Monteiro, Delfim Pedrosa, Sérgio Coelho, Tiago J. C. Sousa, Luís Machado, João L. Afonso, “A Novel Multilevel Solid-State Transformer for Hybrid Power Grids”, IEEE SEST International Conference on Smart Energy Systems and Technologies, Vaasa, Finland, Sept. 2021.

[29] Vítor Monteiro, Tiago J. C. Sousa, Delfim Pedrosa, Sérgio Coelho, João L. Afonso, “A Three-Level dc-dc Converter for Bipolar dc Power Grids: Analysis and Experimental Validation,” IEEE IECON 2020 - Industrial Electronics Conference, Singapore, Oct. 2020.